

Article

Not peer-reviewed version

3D Printing and Supercritical Technologies for the Fabrication of Intricately Structured Aerogels Derived from the Alginate–Chitosan Polyelectrolyte Complex

[Natalia Menshutina](#) , [Andrey Abramov](#) , Eldar Golubev , [Pavel Tsygankov](#) *

Posted Date: 16 May 2025

doi: 10.20944/preprints202505.1195.v1

Keywords: direct ink writing; heterophase system; supercritical process; supercritical sterilization; aerogel



Preprints.org is a free multidisciplinary platform providing preprint service that is dedicated to making early versions of research outputs permanently available and citable. Preprints posted at Preprints.org appear in Web of Science, Crossref, Google Scholar, Scilit, Europe PMC.

Copyright: This open access article is published under a Creative Commons CC BY 4.0 license, which permit the free download, distribution, and reuse, provided that the author and preprint are cited in any reuse.

Disclaimer/Publisher's Note: The statements, opinions, and data contained in all publications are solely those of the individual author(s) and contributor(s) and not of MDPI and/or the editor(s). MDPI and/or the editor(s) disclaim responsibility for any injury to people or property resulting from any ideas, methods, instructions, or products referred to in the content.

Article

3D Printing and Supercritical Technologies for the Fabrication of Intricately Structured Aerogels Derived from the Alginate–Chitosan Polyelectrolyte Complex

Natalia Menshutina, Andrey Abramov, Eldar Golubev and Pavel Tsygankov *

Department of chemical and pharmaceutical engineering, Mendeleev University of Chemical Technology of Russia, Miusskaya pl. 9, 125047 Moscow, Russia

* Correspondence: pavel.yur.tsygankov@gmail.com

Abstract: Additive technologies represent a promising approach to solving problems in the field of tissue engineering, with the potential to develop personalized matrices for the growth of tissue and organ cells. The utilisation of supercritical technologies, encompassing the processes of drying and sterilisation within a supercritical fluid environment, has been demonstrated to generate significant opportunities in the domain of obtaining highly effective matrices for cell growth based on biocompatible materials. The present paper considers the processes involved in the formation of aerogels based on alginate-chitosan polyelectrolyte complex. This paper explores a range of methodologies for the printing process, encompassing direct gel printing and 3D printing employing a heterophase system. The demonstration is made of the possibility of combining the processes of drying and sterilisation in a supercritical fluid environment of personalized matrices based on a polyelectrolyte complex.

Keywords: direct ink writing; heterophase system; supercritical process; supercritical sterilization; aerogel

1. Introduction

At the present time, bioengineering represents a field of great potential in the development of technologies for the creation of matrices that are conducive to the effective growth of tissue and organ cells. These matrices are to be based on biocompatible and biodegradable materials. The utilisation of highly porous materials, such as aerogels, constitutes a salient domain of research. Aerogels are materials with low density (0.003–0.15 kg/m³), an open porous structure (up to 99%) and a high specific surface area (500–1000 m²/g) [1]. It is evident that aerogels possess a number of advantageous properties, which renders them a promising material for use in a variety of applications. These include the cultivation of cells [2], the fabrication of highly effective drug delivery systems [3], the development of energy storage devices [3], the utilisation as catalysts [4,5], the function as sorbents [6,7], and the production of heat and sound insulating materials [8]. However, the formation of a given geometry of aerogels is a rather difficult task due to their low density, high porosity and, as a consequence, low mechanical strength. At present, the method of casting into a mold is employed for the purpose of forming the macrostructure of aerogels; however, this approach is limited in terms of the options available for the final geometry. Moreover, the utilisation of prevalent methodologies for the formation of intricate geometries is often unsuccessful in yielding materials with regulated porosity. The resolution of these issues can be achieved through the implementation of additive manufacturing processes.

The utilisation of additive technologies in the fabrication of aerogels facilitates the realisation of the requisite intricate geometry of the product without the necessity of subsequent post-processing. This development signifies a substantial augmentation in the domains of application in the field of

functional material development, wherein both a developed internal structure and a complex geometry of the product are of paramount importance.

Aerogels derived from biopolymers, including alginate and chitosan, are non-toxic, biocompatible, and biodegradable, thus rendering them suitable for medical applications [9,10] and the pharmaceutical industry [11]. At present, aerogels based on biopolymers have already found their application as hemostatic agents [12,13], highly effective drug delivery systems [14], and in tissue engineering to obtain matrices for the growth of tissue and organ cells [15,16].

Of particular interest is a hybrid gel based on alginate and chitosan [17]. The formation of the hybrid structure is attributable to a chemical reaction between the alginate polyanion and the chitosan polycation, which results in the formation of the corresponding polyelectrolyte complex [18]. The formation of a stable gel based on the alginate-chitosan polyelectrolyte complex has the potential to yield fundamentally new materials, eliminate the use of aggressive cross-linking agents, and enhance thermal, chemical, mechanical properties and increase the stability of materials [19–22].

The development of new materials with strictly defined properties for solving problems in the fields of medicine, pharmaceuticals and biotechnology necessitates the search for effective approaches to achieving their sterility [23–25]. In the contemporary era, a plethora of sterilisation methodologies have been sanctioned by regulatory authorities and are deemed particularly pertinent for implementation in industrial contexts [26]. The methods employed include heat or steam sterilization [27], sterilization with ethylene oxide [28] and gamma irradiation [29]. However, it should be noted that these approaches are associated with certain disadvantages, namely the destructive effect of the sterilising agent on the structure and properties of the final products. This phenomenon is most evident in materials and products derived from biopolymers, hydrophilic compounds and heat-labile substances. Currently, there is a paucity of comprehensive approaches to the sterilisation of products obtained from heat-labile, hydrophilic materials or materials of biological origin. Consequently, there is an imperative need to develop sterilisation methods that operate under mild conditions and do not result in the destruction of the structure of final products.

The utilisation of supercritical technologies holds considerable promise in the domain of sterilising biomedical products. In the context of supercritical sterilization in a carbon dioxide environment, the process parameters are known to vary within the following ranges: pressure from 8 to 40 MPa, temperature from 35 to 90 °C [30–32]. As demonstrated in the research [31,32], experimental evidence has been provided to show that an increase in pressure and temperature can contribute to the inactivation of microorganisms. This is due to an increase in the solubility of carbon dioxide and an acceleration of the process of diffusion into the cell through the plasma membrane. However, an increase in pressure above 10 MPa exerts minimal influence on the solubility of carbon dioxide in water [31]. At pressures approaching or exceeding the critical pressure, an increase in temperature leads to a decrease in density, consequently reducing the dissolving capacity of carbon dioxide [33]. In order to increase the inactivation rate, additional sterilising agents are used in combination with supercritical carbon dioxide. The most effective sterilising agent in the supercritical sterilisation process is hydrogen peroxide, as demonstrated in [32].

The present paper discusses the processes of obtaining matrices for cell growth based on the alginate-chitosan polyelectrolyte complex. In order to form a given geometry of the final product, two 3D printing methods are presented, namely direct gel printing and 3D printing using a heterophase system. The experimental studies demonstrate the key advantages and disadvantages of each of the technologies under consideration. In turn, to preserve the highly porous structure and ensure the sterility of the final products, a combined drying and sterilisation process in a supercritical carbon dioxide environment is presented.

2. Results and Discussion

2.1. Rheological Study of Different “Ink” Composition

The dynamic viscosity of the sodium alginate-chitosan and partially cross-linked sodium alginate-chitosan systems was investigated for all analysed polymer concentrations. In order to ascertain the effect of polymer concentration on the viscosity value, a test was performed at a minimum shear rate of 0.01 s^{-1} (Table 1).

Table 1. Viscosity of sodium alginate-chitosan and partially cross-linked sodium alginate-chitosan systems on chitosan concentration.

Concentration of chitosan, wt.%	Viscosity, $\text{Pa} \cdot \text{s}$	
	Alginate	Partly cross-linked alginate
0,0	0,8	1032,4
0,5	82,2	1446,0
1,0	318,7	1578,2
1,5	1591,3	1754,5
2,0	1800,0	7970,0

In the case of the sodium alginate-chitosan system, an increase in the chitosan concentration leads to a significant increase in viscosity from 0.8 to 1800 Pa·s. This phenomenon can be attributed to an increase in the concentration of the solid phase within the material's volume. Consequently, an elevated stress is necessary to displace the layers of the material, thereby enhancing its viscosity.

A comparable dependence is observed when adding chitosan to the volume of gel material based on partially cross-linked sodium alginate. The maximum viscosity of partially cross-linked sodium alginate is achieved at the maximum concentration of chitosan. The high viscosity of the system has the potential to impede the implementation of layer-by-layer formation of products using the 3D printing process.

One of the factors that must be considered when determining the possibility of using materials for the implementation of the three-dimensional printing process is the flow type [34]. In order to implement the three-dimensional printing process, it is necessary that the source material be characterised by a pseudo-plastic flow type, which is defined by a decrease in viscosity under the action of shear stresses. The present study investigates the rheological properties of gel materials of varying compositions, with a linear increase in shear rate from 0.01 to 100 s^{-1} . The subsequent analysis of the obtained data resulted in the construction of flow curves (Figure 1).

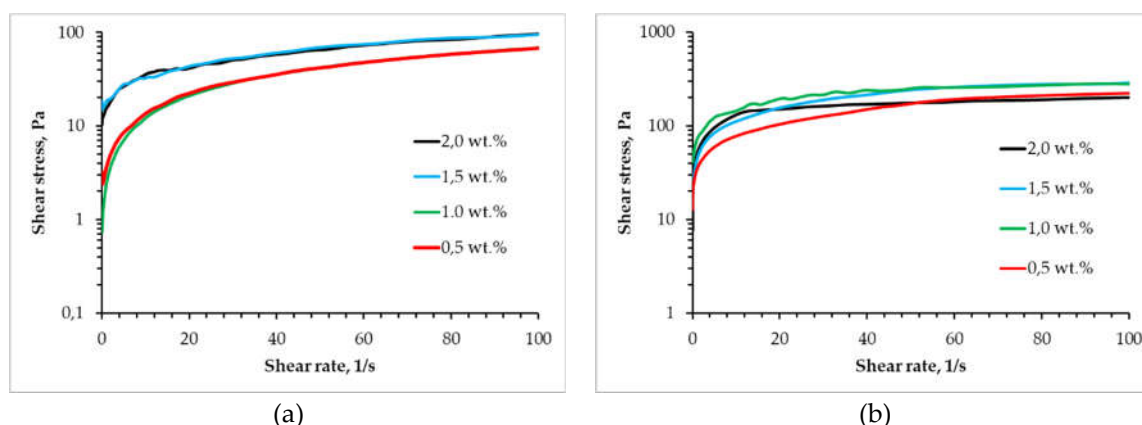


Figure 1. Flow curves for alginate (a) and partly crosslink alginate (b) solution with different concentration of chitosan.

It can be concluded from the results presented that, irrespective of composition, a pseudoplastic flow type is observed, i.e. an increase in stress with an increase in shear rate. It is noteworthy that the degree of pseudoplasticity, i.e. the deviation of the system from ideality, increases in proportion to

the increase in the concentration of chitosan, for both the sodium alginate-chitosan systems and the partially cross-linked sodium alginate-chitosan systems.

A quantitative assessment of the thixotropic properties of the obtained systems was conducted, with an increase in the shear rate from 0.01 s⁻¹ to 100 s⁻¹ and a subsequent decrease in the shear rate from 100 to 0.01 s⁻¹. As demonstrated by the extant research, thixotropy curves were plotted in the shear stress-shear rate coordinates (see the supplementary materials).

It was observed that all the obtained compositions of the materials “sodium alginate-chitosan” and “partially cross-linked sodium alginate-chitosan” exhibited a thixotropy hysteresis loop. It has been demonstrated that the thixotropic properties of a system, i.e. its capacity for recovery, are optimised when the area of the hysteresis loop is minimised. The areas of the hysteresis loops were determined for all the compositions (Table 2).

Table 2. Areas of thixotropy hysteresis loops of the “sodium alginate-chitosan” and “partially cross-linked sodium alginate-chitosan” systems depending on the chitosan concentration.

Concentration of chitosan, wt.%	Thixotropy hysteresis loops	
	Alginate	Partly cross-linked alginate
0,0	9,5	2374,2
0,5	29,9	2405,8
1,0	40,2	2416,1
1,5	105,8	2887,9
2,0	659,3	2967,8

The sodium alginate-chitosan systems have been shown to exhibit reduced values for the hysteresis loop area. It has been demonstrated that an increase in the concentration of chitosan results in an increase in the hysteresis loop area, and consequently, a slower recovery of the initial viscosity. It has been demonstrated that partial cross-linking of sodium alginate results in a substantial reduction in thixotropic properties, as evidenced by an augmentation in the hysteresis loop area.

In order to ascertain the viability of employing the obtained systems for the purpose of 3D printing, studies were conducted with the objective of determining the flow onset point during extrusion. The material’s capacity to transition from an elastically deformable body to a viscous liquid under the influence of shear stresses is determined by the presence of the flow onset point. The occurrence of this transition is determined by the presence of the yield point, defined as the intersection of the storage modulus and loss modulus curves.

The viscoelastic behaviour of partially cross-linked sodium alginate solutions was the focus of the study, which was conducted at a constant angular frequency of 10 rad/s. In accordance with the findings of this study, the storage modulus and loss modulus curves were subsequently constructed for the entirety of the systems obtained. For instance, Figure 2 illustrates the dependences for a chitosan concentration of 1.5 wt.%. (All curves can be found in the supplementary materials).

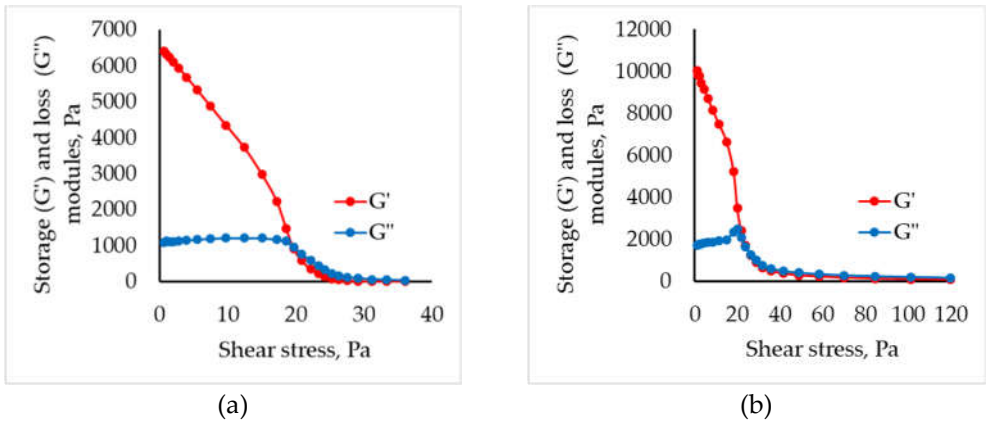


Figure 2. Storage (G') and loss (G'') modulus for alginate (a) and partly crosslinked alginate (b) solution with 1,5 wt.% of chitosan.

The values of shear stresses required to initiate flow in the studied systems are presented in Table 3.

Table 3. Values of shear stresses required to initiate the flow of the studied systems “sodium alginate-chitosan” and “partially cross-linked alginate-chitosan”.

Concentration of chitosan, wt. %	Shear stresses	
	Alginate	Partly cross-linked alginate
0,0	0	77
0,5	0,8	42,8
1,0	1,8	32,3
1,5	19,7	26,3
2,0	52,8	12,2

Based on the obtained results, it was established that the addition of chitosan particles to the sodium alginate solution leads to a shift in the flow initiation point. In turn, for materials based on partially cross-linked sodium alginate, a decrease in the required stress is observed with an increase in the chitosan concentration. This dependence may be due to an increase in the amount of solid phase in the system structure and, presumably, incomplete wettability of chitosan particles, which in turn leads to instability and, as a consequence, a decrease in the stresses required to initiate the flow initiation.

It was determined that the addition of chitosan to a sodium alginate solution resulted in an increase in viscosity of the system, a decrease in thixotropic properties, and a shift in the flow onset point to a region of greater deformations. Conversely, when systems are formed based on partially cross-linked sodium alginate, the addition of chitosan results in an increase in viscosity and a decrease in thixotropic properties, analogous to materials based on non-cross-linked sodium alginate. However, it should be noted that for the “partially cross-linked sodium alginate-chitosan” systems, the flow onset point shifts to the region of smaller deformations with an increase in the chitosan concentration, which is presumably due to the incomplete wettability of chitosan particles. Subsequently, the resulting “sodium alginate-chitosan” and “partially cross-linked sodium alginate-chitosan” systems were studied as viscous “ink” for the implementation of extrusion 3D printing.

2.2. Investigation of 3D-Printing Process

The formation of the product by applying ink to the working surface represents a conventional approach to 3D printing. In such instances, it is imperative that the ink exhibits rapid viscosity recovery and does not exhibit any spreading after the extrusion process. An alternative approach involves the formation of the product in the volume of a heterophase system. The heterophase system provides support for the product during printing and allows for an expansion of the range of “ink” for the process. Gelatin microparticles were utilised as a heterophase system [35]. The parameters for the printing process, when implementing each of the technologies under consideration, are presented in Section 4.3.

In the course of the conducted experimental studies it was established that for the implementation of the 3D printing process with the formation of the product by applying ink to the working surface, the necessary rheological characteristics are possessed by gel materials based on partially cross-linked sodium alginate with chitosan concentrations from 0.5 to 1.5 wt.%.

When implementing the printing process using sodium alginate and chitosan concentrations from 0.5 to 1.5 wt.%, spreading of the material over the surface of the working area is observed due to insufficient viscosity and low stress values necessary to initiate the flow of gel materials. To use

gel materials based on the sodium alginate-chitosan system with a chitosan concentration of up to 1.5 wt.% as “ink”, it is necessary to use the 3D printing process with the formation of the product in the volume of the heterophase system, which prevents the spreading of materials after the extrusion process.

In all cases, an increase in the chitosan concentration to 2 wt.% results in the extruder nozzle becoming clogged due to the high viscosity of the system and the high solid phase content. It is evident that the implementation of the 3D printing process using the developed gel material compositions is most affected by the solid phase (chitosan) concentration, the solution viscosity, and the flow onset point. The implementation of the 3D printing process, involving the application of ink to the working surface to form a product, imposes more stringent requirements on the ink. From the standpoint of the thixotropic properties of the obtained printing compositions, the range of thixotropy hysteresis loop areas from 2300 to 2900 is deemed acceptable and ensures effective viscosity recovery after extrusion of gel materials onto the surface of the working area.

2.3. Integrated Supercritical Drying and Sterilization Processes

The objects selected for the study of the combined processes of supercritical drying and sterilization were products of complex geometry formed within the volume of a heterophase system. Sodium alginate-chitosan systems were utilised as ink. In order to address the issue of the final products’ shape, the 3D objects that had been printed were subjected to a freezing process. The frozen samples were stored in a 0.5 M hydrochloric acid solution at ambient temperature for a 24-hour period. This stage is necessary for the dissolution of the chitosan particles. It has been established that, as a consequence of a chemical reaction, a polyelectrolyte complex of alginate and chitosan is formed during the dissolution process. This reaction is characterised by the binding of the carboxyl groups of alginate and the amine groups of chitosan. During this stage, a stable gel is formed (Figure 4).

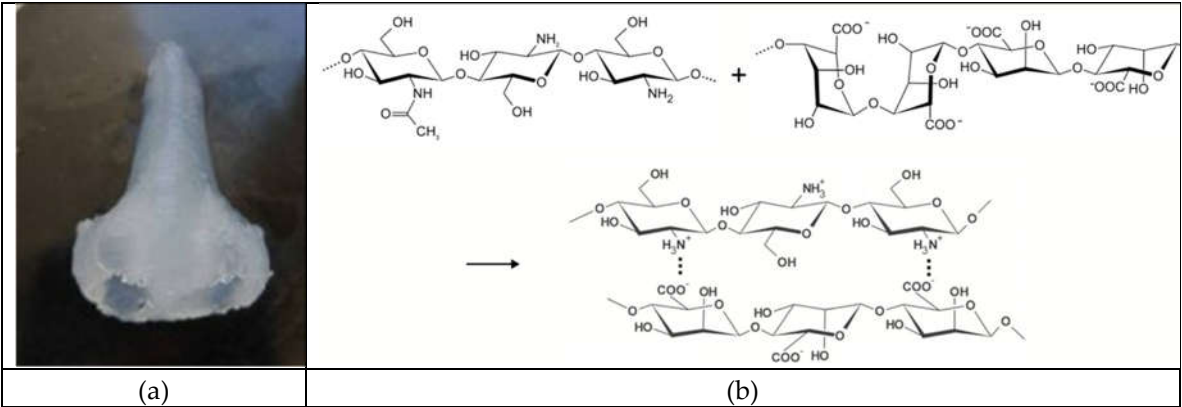


Figure 4. 3D-printed object based on “algininate-chitosan” solution with 1,5 wt% concentration of chitosan after gelation process (a); mechnism of polyelectroly complex formation (b).

Subsequent to the completion of the gelation process, the solvent was gradually replaced with isopropyl alcohol in order to carry out the supercritical drying and sterilization process.

In accordance with the developed process flow chart and the design of the devices, following the completion of the supercritical drying process, the supercritical fluid sterilization process was carried out using an additional sterilizing agent, hydrogen peroxide.

The efficiency of the sterilisation process was assessed in accordance with GMP OFS 1.2.4.0003.15 Sterility. The nutrient medium employed for sterility testing was obtained by first dissolving 31 g of dry thioglycollate medium powder in 1 l of distilled water. This was then boiled for 2 minutes and subsequently filtered. The resulting thioglycollate medium was then titrated with an HCl solution to a pH of 7.10. The medium was then transferred to sterile flasks sealed with cotton-

gauze stoppers and sterilised in a Stegler VK-18 autoclave at 121°C and an excess pressure of 1 atm for 15 minutes.

Following the conclusion of the supercritical sterilization process at varying mass flow rates of carbon dioxide, the materials were transferred to flasks containing a nutrient medium under sterile conditions. The work was conducted within a Biosan UVC/T-B-AR PCR box, equipped with a UV recirculator. Subsequently, the flasks containing the materials were placed in a thermostat and maintained at a temperature of 37°C for a period of 14 days.

The results were recorded visually on a daily basis during the 14-day incubation period. The presence of microbial growth was assessed by the appearance of turbidity, individual spherical colonies and other microscopic changes in the medium. The presence of microorganisms was confirmed through microscopic analysis.

The experimental studies confirmed the sterility of the final materials under the selected process parameters.

2.4. Analytical Study of Hybryd Aerogel Based on Polyelectrolyte Complex

As illustrated in Figure 5, the images depict aerogels derived from a polyelectrolyte complex of alginate and chitosan. The samples were obtained through the utilisation of sodium alginate-chitosan ink, which was subsequently printed within the volume of the heterophase system. Notably, the sample exhibiting a chitosan concentration of 2 mass% was obtained without the employment of three-dimensional printing techniques. These images were obtained through the use of scanning electron microscopy (SEM).

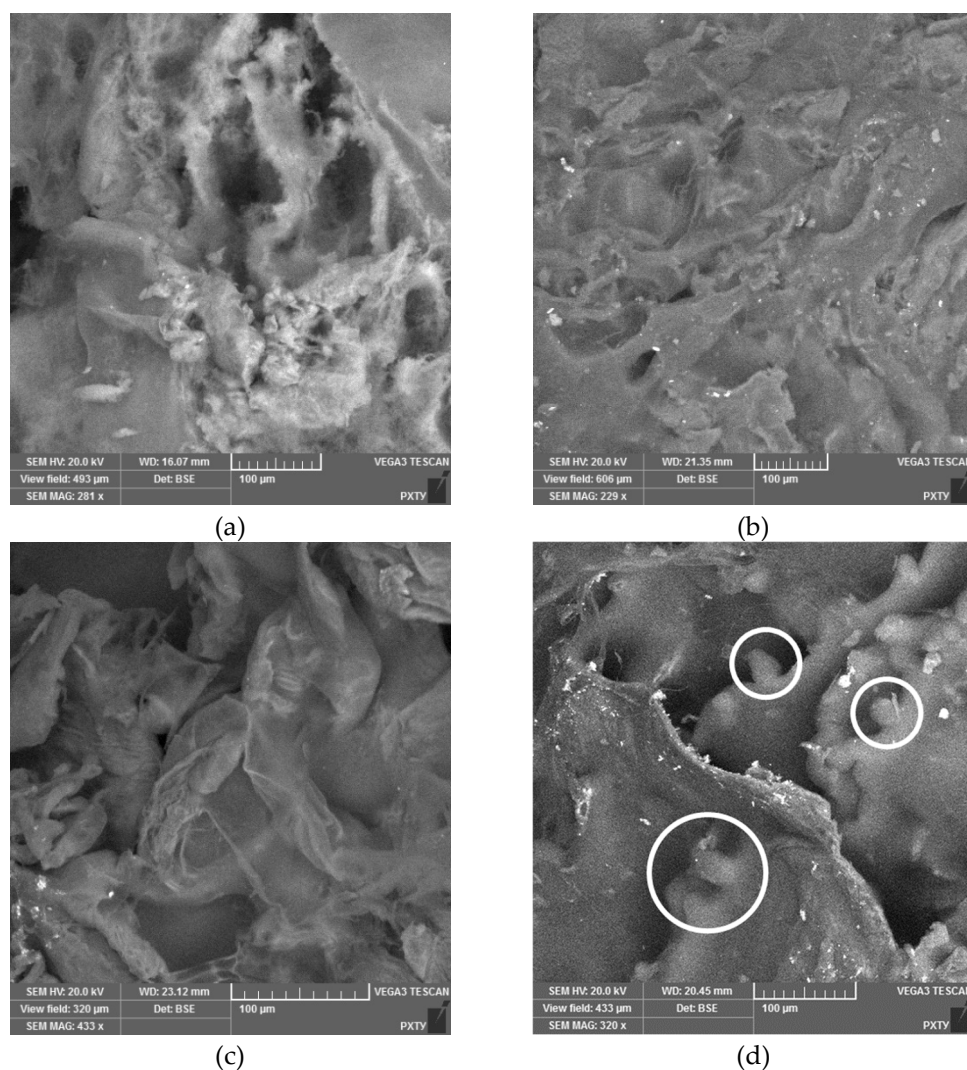


Figure 5. Images of the internal structure of aerogels based on a polyelectrolyte complex with different chitosan content: a) 0.5 wt.%; b) 1 wt.%; c) 1.5 wt.%; d) 2 wt.%.

As the concentration of chitosan increases, the resulting SEM images demonstrate that a more heterogeneous structure is formed. For the sample with a chitosan concentration of 2 wt.%, areas are identified that presumably represent chitosan particles coated with a polyelectrolyte shell. The formation of a heterogeneous structure is associated with the features of the process of obtaining the polyelectrolyte complex. The dissolution of chitosan particles is initiated upon contact with a hydrochloric acid solution.

In order to study the formation of the polyelectrolyte complex after the printing process, gelation and drying in a supercritical fluid medium, IR spectroscopy studies were carried out. As illustrated in Figure 6, the IR spectra of the initial sodium alginate and chitosan powders are presented. The spectrum of chitosan displays a broad band ranging from approximately 3000 to 3600 cm^{-1} , indicative of the stretching vibrations of O–H and N–H bonds. The maximum at wave numbers of $\sim 2860 \text{ cm}^{-1}$ corresponds to vibrations of the C–H bonds of all hydrocarbon components. The peak observed at 1590 cm^{-1} is attributed to the overlap of the peaks belonging to the C–O and N–H groups.

The spectrum of sodium alginate is characterised by a broad band with a peak at $\sim 3220 \text{ cm}^{-1}$, which corresponds to the O–H stretching vibrations. The presence of two peaks at $\sim 1590 \text{ cm}^{-1}$ and $\sim 1400 \text{ cm}^{-1}$ is attributed to the carboxyl group. At $\sim 1020 \text{ cm}^{-1}$, C–O–C vibrations are observed.

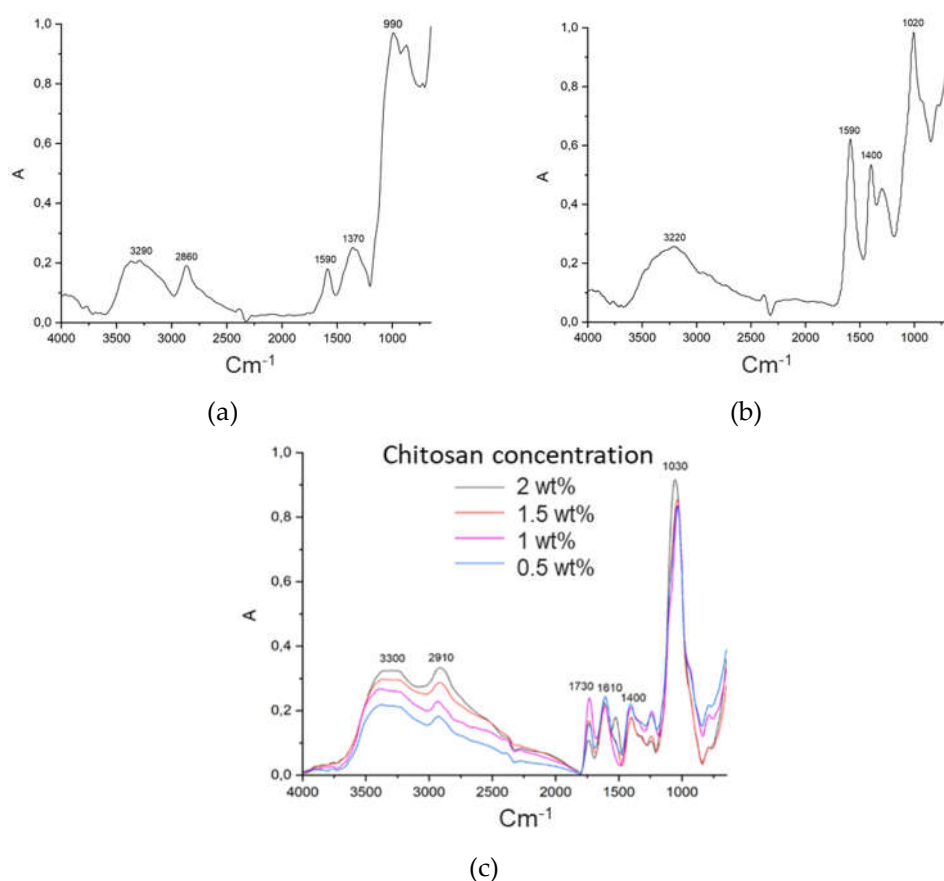


Figure 6. IR spectra of a) chitosan; b) sodium alginate; c) aerogel based on polyelectrolyte complex.

The IR spectra of the obtained aerogels demonstrate the formation of a polyelectrolyte complex. The polyelectrolyte complex exhibits a more intense absorption band at $\sim 3300 \text{ cm}^{-1}$, attributable to the formation of hydrogen bonds between the –OH and –NH₂ groups in chitosan and the –C=O and –OH groups of sodium alginate. New peaks at approximately 1610 cm^{-1} and 1730 cm^{-1} were observed for all four alginate:chitosan ratios. The peak at 1610 cm^{-1} exhibits comparable intensity in all four

samples. The peak at 1730 cm⁻¹ corresponds to the asymmetric stretching of the –COO– groups, thus confirming the formation of a polyelectrolyte complex.

Table 4 presents the characteristics of aerogels based on the polyelectrolyte complex alginate – chitosan: true density ($\rho_{\text{ист}}$), apparent density ($\rho_{\text{каж}}$), porosity, BET specific surface area ($S_{\text{БЕТ}}$), Barrett-Joyner-Halenda pore volume (V_{BDH}).

Table 4. Characteristics of aerogels based on the polyelectrolyte complex sodium alginate – chitosan.

Concentration of chitosan, wt. %	$\rho_{\text{ист}}$, g/cm ³	$\rho_{\text{каж}}$, g/cm ³	Porosity, %	$S_{\text{БЕТ}}$, m ² /g	V_{BDH} , cm ³ /g
0,5	1.684	0.090	95	238	1.23
1,0	1.853	0.099	95	199	0.59
1,5	1.884	0.076	96	153	0.64
2,0	1.982	0.062	97	108	0.37

An increase in the concentration of chitosan has been shown to result in an increase in true density, which in turn provides a reinforcing effect and a decrease in apparent density of the samples. It has been demonstrated that an increase in the concentration of chitosan results in a decrease in the specific surface area and volume of mesopores. This phenomenon is associated with the formation of a non-uniform structure and incomplete dissolution of chitosan.

Consequently, supercritical drying facilitates the production of hybrid aerogels derived from the polyelectrolyte complex sodium alginate-chitosan. The process of supercritical drying has been demonstrated to be an effective method for ensuring the preservation of the structural integrity of products obtained through the 3D printing process. The process of supercritical sterilization does not result in the degradation of the porous structure of the final products and allows the achievement of sterility.

3. Conclusions

The present study investigates the processes involved in the formation of aerogels of complex geometry based on the polyelectrolyte complexes sodium alginate-chitosan, utilising additive and supercritical technologies. A comprehensive study of the rheological properties of materials based on sodium alginate and partially cross-linked sodium alginate with the addition of chitosan was carried out in order to set the complex geometry of the final products. The rheological studies demonstrated that all the developed gel compositions exhibited a pseudo-plastic flow character, whereby an increase in the shear rate resulted in an increase in shear stress and a decrease in effective viscosity. The concentration of the dispersed phase (chitosan particles) has been demonstrated to result in a significant increase in the viscosity of the analysed systems from 0.8 to 1800.0 Pa·s for sodium alginate solutions and from 1032 to 7970.0 Pa·s for partially cross-linked sodium alginate. Furthermore, all analysed compositions of viscous “ink” are characterised by the presence of thixotropic properties, that is, the ability of the gel structure to partially collapse under shear and recover after the load is removed. It is noteworthy that an increase in the concentration of chitosan results in a reduction of the thixotropic properties, both for sodium alginate solutions and for solutions of partially cross-linked sodium alginate.

Based on the conducted studies of the rheological properties of viscous “ink” and experimental studies of the 3D printing process, it was found that viscous “ink” based on partially cross-linked alginate with a chitosan content of 0.5–1.5 wt.% is optimal for implementing the direct gel printing process. These compositions have sufficient viscosity and a pronounced yield point, as well as relatively fast structural relaxation (hysteresis loop of about 2400–2700), which prevents layer spreading and ensures the preservation of the geometry of the final products. In turn, for sodium alginate solutions with different chitosan content, the possibility of implementing the printing process using a heterophase system based on gelatin was shown.

For the products obtained in the volume of the heterophase system, a study of combined drying and sterilization processes in a supercritical carbon dioxide environment was carried out. Complex analytical studies demonstrated the formation of a highly porous structure of the final products with a high specific surface area (up to 238 m²/g) and a high specific pore volume (up to 1.23 cm³/g). It is worth noting that an increase in the chitosan concentration to 2 wt% worsens the structural characteristics of the materials due to the formation of a heterogeneous structure, which is confirmed by scanning electron microscopy images. Thus, the implementation of combined drying and sterilization processes made it possible to achieve sterility of the final products without deformation of the internal structure and geometry of the products.

In this work, an approach to the implementation of processes for obtaining highly porous matrices with complex geometry using additive and supercritical technologies is proposed. The potential for producing sterile aerogels based on the sodium alginate-chitosan polyelectrolyte complex using various additive manufacturing (direct gel printing and 3D printing using a heterophase system) and combined drying and sterilisation processes in a supercritical carbon dioxide environment has been demonstrated.

4. Materials and Methods

4.1. Materials

Gelatin (CAS Number: 9000-70-8, Merck KGaA, Germany) and anhydrous calcium chloride (RusChem, Moscow, Russia) were used to obtain a heterophase system. Alginic acid sodium salt (CAS Number: 9005-38-3, Sigma-Aldrich, USA) and chitosan (CAS Number: 9005-38-3, Sigma-Aldrich, USA) was used as an ink precursor. Other materials, including distilled water, isopropanol and hydrogen peroxide (36 wt.%), were purchased from RusChem (Moscow, Russia). Carbon dioxide with a purity of >99% was used for supercritical drying and sterilization.

4.2. Methods of "Ink" and Heterophase System Preparation

As demonstrated in [34], the optimal properties for the implementation of the printing process are exhibited by material compositions with a sodium alginate concentration of 2 wt.%. The concentration of chitosan in the materials for printing varied: 0; 0.5; 1; 1.5 and 2 wt.%. In this work, two schemes for obtaining viscous "ink" for the implementation of the three-dimensional printing process are proposed, depending on the selected technology.

4.2.1. 3D Printing Process Utilizing Heterophase System

In the implementation of 3D printing technology utilising a heterophase system, the process of acquiring viscous "ink" derived from sodium alginate and chitosan entails the generation of a sodium alginate solution in distilled water, employing a rotor-stator homogenizer (IKA Ultra-Turrax T 25 digital) at a rotor speed of 9000 rpm and a process duration of 2 minutes. Following the complete dissolution of sodium alginate in the resulting solution, the dispersion of the chitosan powder is carried out at a rotor speed of 12,000 rpm and a process time of 5 minutes. The values selected for the speed and time of the dispersion process are due to the necessity of achieving a uniform distribution of the chitosan powder throughout the volume of the solution.

4.2.2. Direct Ink Writing (DIW)

In the implementation of the direct gel printing technology, a modified solution of partially cross-linked sodium alginate was utilised. Calcium chloride is dissolved in distilled water until a concentration of 0.2 wt.% is reached, using a magnetic stirrer. Chitosan powder is dispersed in the resulting solution by means of a rotor-stator homogenizer, with a rotor speed of 12,000 rpm and a process time of 5 minutes, until the required concentration is reached. Subsequently, sodium alginate powder with a 2 wt.% is dispersed.

4.2.3. Heterophase System Preparation

To implement the 3D printing process using a modernized 3D printer construction, a method for obtaining a gelatin-based heterophase system was developed. A given amount of gelatin (4.5wt.%) is dissolved in a solution of calcium chloride with a concentration of 11 mM at a temperature of 60°C, followed by solidification at a temperature of 4°C for 1 hour. The resulting solution is dispersed in an 11 mM calcium chloride solution in a 3:7 volume ratio using a rotor-stator homogenizer (IKA Ultra-Turrax T 25 digital) at a rotor speed of 9000 rpm for 90 seconds. The resulting suspension is centrifuged (Sigma 2-16 PK) at 4°C to remove dissolved gelatin. The centrifugation process continues until a clear solution is obtained over the precipitate. Gelatin microparticles obtained as a result of repeated washing are used as a heterophase system for 3D printing.

4.3. Implementation of 3D Printing Process

In this study, a 3D printer of our own design was utilised to implement the 3D printing process (Figure 7).

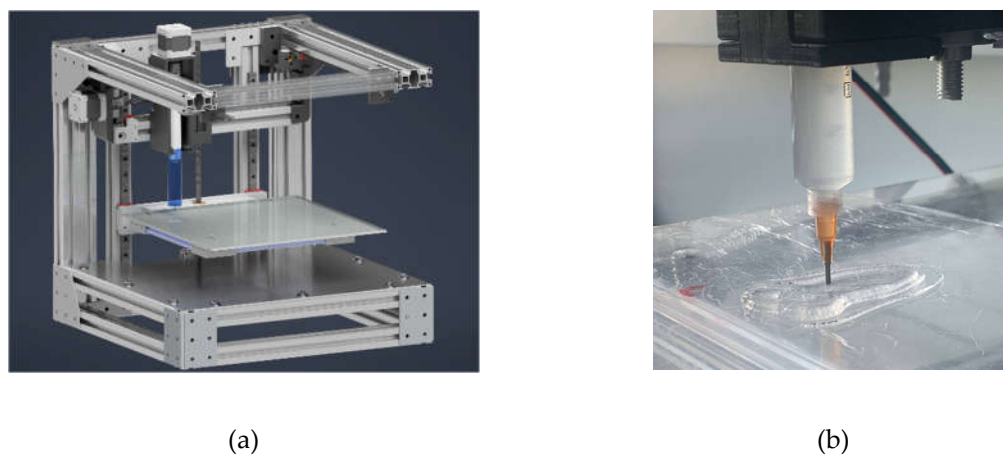


Figure 7. Construction of 3D printer to implement 3D-printing process (a), example of implementation of 3D printing process using direct ink writing technology (b).

The extruder of gel materials proposed in the work was used as a pressing device. [34] (Figure 8).

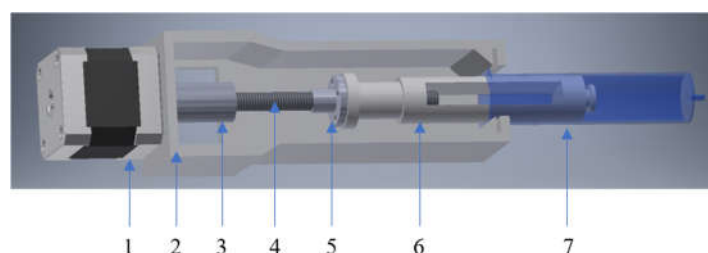


Figure 8. The assembly of the viscous “ink” extruder comprises the following components: 1- stepper motor, 2- housing, 3- coupling sleeve, 4- trapezoidal screw, 5- trapezoidal nut, 6- piston, 7- container for viscous “ink”.

In light of the disparate viscosity characteristics exhibited by the formulated ink compositions, the subsequent process parameters were employed in the implementation of direct gel printing technology: layer thickness 1 mm, extruder nozzle speed 5 mm/s, extruder piston speed 0.1 mm/s, and printing temperature 20 °C. The following parameters were utilised in the implementation of the 3D printing process using a heterophase system: layer thickness 0.6 mm, extruder nozzle speed 6 mm/s, extruder piston speed 0.01 mm/s, and printing temperature 20 °C.

4.4. Integrated Supercritical Drying and Sterilization Processes

In order to implement the combined processes of drying and sterilisation in a supercritical carbon dioxide environment, a laboratory setup with a high-pressure apparatus with a volume of 70 ml (for loading gel samples) and a cell of 22 ml (for the sterilising agent) was utilised. The fundamental technological scheme and design of the apparatus are presented in Figure 9.

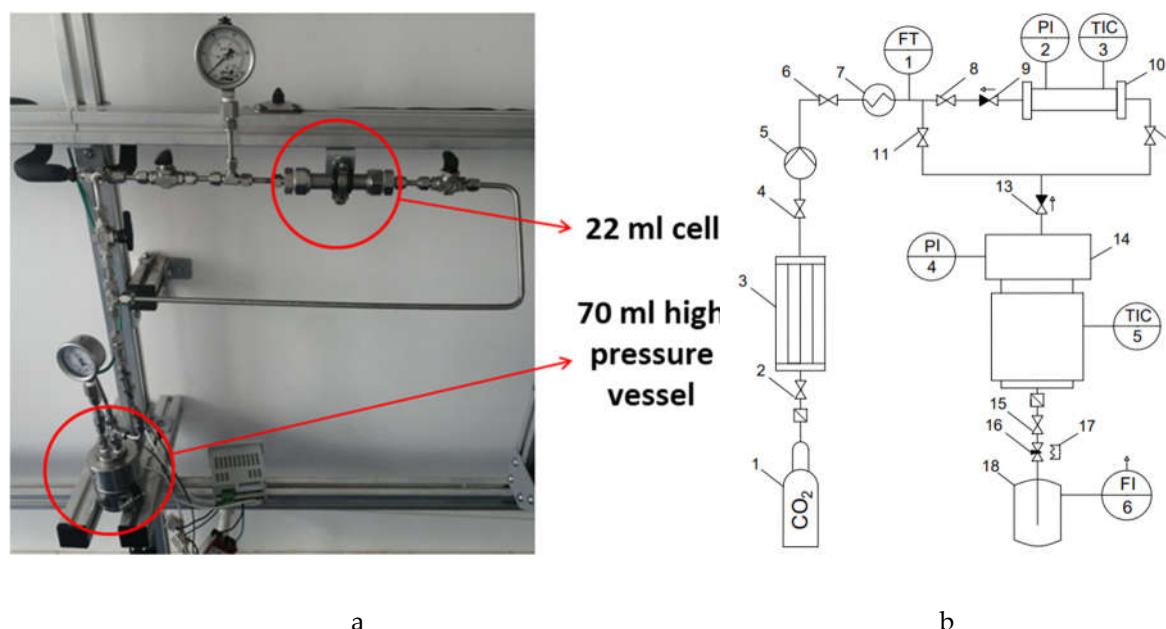


Figure 9. External appearance (a) and flowsheet (b) of the unit for combined processes of supercritical drying and sterilization: 1 – cylinder with carbon dioxide; 3 – condenser; 5 – pump; 7 – heat exchanger; 10 – cell 22 ml; 14 – high-pressure apparatus 70 ml; 17 – heating element; 18 – separator; 2, 4, 6, 8, 11, 12, 15 – shut-off valves; 9, 13 – check valves; 16 – regulating valve; FT1 – Coriolis flow meter; PI2, PI4 – pressure sensors; TIC3, TIC5 – temperature sensors and controllers; FI6 – rotameter.

The valves 8, 11 and 12 ensure the switching of the drying and sterilisation processes. At the initial moment of time, the necessary parameters for conducting combined processes are set in the high-pressure apparatus 14 and the intermediate tank 10. It has been established that the process of dissolving hydrogen peroxide in supercritical carbon dioxide occurs in intermediate tank 10 during the drying process, which occurs in a flow mode. Subsequent to the conclusion of the drying process, valve 11 is closed, whilst valves 8 and 12 are opened in order to conduct the supercritical sterilization process with an additional sterilizing agent in a flow mode.

The supercritical drying process was conducted under the following parameters: temperature 40°C, pressure 120-140 bar, carbon dioxide flow rate 1000 g/h, process time 4-5 h. Upon completion of the process, the pressure is released at a rate of 4 bar/min.

Based on previous studies, the process of supercritical sterilization of aerogels based on the sodium alginate-chitosan polyelectrolyte complex was carried out at a mass flow rate of 500 g/h and a process time of 30 minutes in a flow mode through a cell with H₂O₂, a pressure of 120 bar and a temperature of 40 °C.

4.5. Analytical Study

The nitrogen adsorption-desorption isotherms were measured at -196 °C using a volumetric apparatus (ASAP 2020, Micromeritics, Norcross, GA, USA). The specific surface area was calculated using the BET method for isotherm linear range, and the total sorption mesopore volume was obtained at P/P₀ = 0.95. Pore diameters were determined using the Barrett-Joyner-Halenda (BJH)

algorithm. The BJH algorithm uses a modified Kelvin equation to link the removed adsorbed material from pores with the pore sizes.

Scanning electron microscopy imaging was performed on an SEM (JSM 6510 LV, JEOL, Akishima, Japan).

The determination of the viscosity characteristics was carried out on an Anton Paar MCT 302 rheometer with a plane–plane measuring unit type with a diameter of 25 mm and a temperature of 20 °C. In order to enhance the precision of the measurements and mitigate the impact of thixotropic properties on the outcomes, a relaxation time of 10 minutes was established for all studies.

Supplementary Materials: The following supporting information can be downloaded at the website of this paper posted on Preprints.org.

Author Contributions: Conceptualization, N.M. and A.A.; methodology, P.T. and A.A.; investigation, P.T. and E.V.; project administration, N.M.; writing—original draft preparation, P.T. and A.A. All authors have read and agreed to the published version of the manuscript.

Funding: This research was funded by the Russian Science Foundation, grant number 23-73-01216.

Conflicts of Interest: The authors declare no conflict of interest. The funders had no role in the design of the study; in the collection, analyses, or interpretation of data; in the writing of the manuscript; or in the decision to publish the results.

References

- Smirnova I., Gurikov P. Aerogel production: Current status, research directions, and future opportunities // *The Journal of Supercritical Fluids*. – 2018. – Vol. 134. – Pp. 228-233.
- Zhao S., Malfait W. J., Guerrero-Alburquerque N., Koebel M. M., Nyström G. Biopolymer aerogels and foams: Chemistry, properties, and applications // *Angewandte Chemie International Edition*. – 2018. – Vol. 57, 26. – Pp. 7580-7608.
- Ambrosi A., Pumera M. 3D-printing technologies for electrochemical applications // *Chemical Society Reviews*. – 2016. – Vol. 45, 10. – Pp. 2740-2755.
- Maleki H., Hüsing N. Current status, opportunities and challenges in catalytic and photocatalytic applications of aerogels: Environmental protection aspects // *Applied Catalysis B: Environmental*. – 2018. – Vol. 221. – Pp. 530-555.
- Shaari N., Kamarudin S. K. Current status, opportunities, and challenges in fuel cell catalytic application of aerogels // *International Journal of Energy Research*. – 2019. – Vol. 43, 7. – Pp. 2447-2467.
- Shin J. H., Heo J.-H., Jeon S., Park J. H., Kim S., Kang H.-W. Bio-inspired hollow PDMS sponge for enhanced oil–water separation // *Journal of hazardous materials*. – 2019. – Vol. 365. – Pp. 494-501.
- Maleki H. Recent advances in aerogels for environmental remediation applications: A review // *Chemical Engineering Journal*. – 2016. – Vol. 300. – Pp. 98-118.
- Xu X., Zhang Q., Hao M., Hu Y., Lin Z., Peng L., Wang T., Ren X., Wang C., Zhao Z. Double-negative-index ceramic aerogels for thermal superinsulation // *Science*. – 2019. – Vol. 363, 6428. – Pp. 723-727.
- Muñoz-Ruiz A. Synthesis and Characterization of a New Collagen-Alginate Aerogel for Tissue Engineering / Muñoz-Ruiz A., Escobar-García D.M., Quintana M., Pozos-Guillén A., Flores H. // *Journal of Nanomaterials*. – 2019. – T. 2019. DOI: 10.1155/2019/2875375
- Obaidat R.M. Drying Using Supercritical Fluid Technology as a Potential Method for Preparation of Chitosan Aerogel Microparticles / Obaidat R.M., Tashtoush B.M., Bayan M.F., T. Al Bustami R., Alnaief M. // *AAPS PharmSciTech*. – 2015. – T. 16, № 6. – C. 1235–1244. DOI: 10.1208/s12249-015-0312-2
- Santos-López G. Aerogels from Chitosan Solutions in Ionic Liquids / Santos-López G., Argüelles-Monal W., Carvajal-Millan E., López-Franco Y.L., Recillas-Mota M.T., Lizardi-Mendoza J. // *Polymers*. – 2017. – T. 9, № 12. – C. 722. DOI: 10.3390/polym9120722
- Mecwan M. Recent advances in biopolymer-based hemostatic materials / Mecwan M., Li J., Falcone N., Ermis M., Torres E [и др.] // *Regenerative Biomaterials*. – 2022. – T. 9. DOI: 10.1093/rb/rbac063

13. Kushwaha R. Biopolymers as Topical Haemostatic Agents: Current Trends and Technologies / Kushwaha R., Sharma S., Kumar S., Kumar A. // Materials Chemistry Horizons. – 2023. – T. 2, № 1. – C. 11–39. DOI: 10.22128/MCH.2022.612.1029
14. Lovskaya D.D. Aerogels as drug delivery systems: In vitro and in vivo evaluations / Lovskaya D.D., Lebedev A.E., Menshutina N. V. // The Journal of Supercritical Fluids. – 2015. – T. 106. – C. 115–121. DOI: 10.1016/j.supflu.2015.07.011
15. Okutucu B. The medical applications of biobased aerogels: ‘Natural aerogels for medical usage’ / Okutucu B. // Medical Devices & Sensors. – 2021. – T. 4, № 1. – C. e10168. DOI: 10.1002/mds3.10168
16. Singh A.K. Fabrication and investigation of physicochemical and biological properties of 3D printed sodium alginate-chitosan blend polyelectrolyte complex scaffold for bone tissue engineering application / Singh A.K., Pramanik K. // Journal of Applied Polymer Science. – 2023. – T. 140, № 12. – C. e53642. DOI: 10.1002/app.53642
17. Rinaudo M. Chitin and chitosan: Properties and applications / Rinaudo M. // Progress in Polymer Science. – 2006. – T. 31, № 7. – C. 603–632. DOI: 10.1016/j.progpolymsci.2006.06.001
18. Wegrzynowska-Drzymalska K. Crosslinking of Chitosan with Dialdehyde Chitosan as a New Approach for Biomedical Applications / Wegrzynowska-Drzymalska K., Grebicka P., Mlynarczyk D.T. [и др.] // Materials. – 2020. – T. 13, № 15. – C. 3413. DOI: 10.3390/ma13153413
19. Gabriele F. Ionic and covalent crosslinking in chitosan-succinic acid membranes: Effect on physicochemical properties / Gabriele F., Donnadio A., Casciola M., Germani R., Spreti N // Carbohydrate Polymers. – 2021. – T. 251. – C. 117106. DOI: 10.1016/j.carbpol.2020.117106
20. Kulig D. Study on Alginate–Chitosan Complex Formed with Different Polymers Ratio / Kulig D., Zimoch-Korzycka A., Jarmoluk A., Marycz K. // Polymers 2016, Vol. 8, Page 167. – 2016. – T. 8, № 5. – C. 167. DOI: 10.3390/polym8050167
21. Gierszewska M. pH-responsive chitosan/alginate polyelectrolyte complex membranes reinforced by tripolyphosphate / Gierszewska M., Ostrowska-Czubenko J., Chrzanowska E. // European Polymer Journal. – 2018. – T. 101. – C. 282–290. DOI: 10.1016/j.eurpolymj.2018.02.031
22. Li Z. Chitosan–alginate hybrid scaffolds for bone tissue engineering / Li Z., Ramay H.R., Hauch K.D., Xiao D., Zhang M. // Biomaterials. – 2005. – T. 26, № 18. – C. 3919–3928. DOI: 10.1016/j.biomaterials.2004.09.062
23. Morozov AM, Morozova AD, Belyak MA, Zamana YuA, Zhukov SV Infections associated with the provision of health care. A modern view of the problem // Bulletin of new medical technologies. 2022. No. 4. P. 107-116.
24. Garmanov S. Yu., Nurislamova GR, Fatkhullin RR, Goryunova SM Cross-contamination in chemical and pharmaceutical production: problems of standardization and unification of requirements // Actual problems of our time. 2006. No. 6. P. 294-305.
25. Fedotov AE Production of sterile drugs // Pharmaceutical technologies and packaging. 2014. No. 9 (247). P. 38-41.
26. Burak L.Ch. Modern methods of preservation used in the food industry // The scientific heritage. 2022. No. 89. P. 106-124.
27. Tapal'skiy D.V., Osipov V.A., Sukhaya G.N., Yarmoolenko M.A., Rogachev A.A., Rogachev A.V. Biocompatible composite antibacterial coatings for protecting implants from microbial biofilms // Problems of health and ecology. 2013. Vol. 36. No. 2. P. 129-134.
28. Nemoikina A.L., Babkina O.V., Alekseenko K.V., Vaitulevich E.A. Study of the influence of ethylene oxide sterilization modes on the properties of glycolide-lactide threads // Bulletin of Tomsk State University. 2014. No. 382. P. 230-233.
29. Vorobyov V., Bozhkova S.A., Tikhilov R.M., Cherny A.Zh. Modern methods of processing and sterilization of allogenic bone tissues (literature review) // Traumatology and Orthopedics of Russia. 2017. Vol. 23. No. 3. P. 134-147.
30. Hossain Md.S., Nik Norulaini N.A., Banana A.A., Mohd Zulkhairi A.R., Ahmad Naim A.Y., Mohd Omar A.K. Modeling the supercritical carbon dioxide inactivation of Staphylococcus aureus, Escherichia coli and Bacillus subtilis in human body fluids clinical waste // Chemical Engineering Journal. 2016. V. 296. P. 173-181.

31. Furukawa S., Watanabe T., Koyama T., Hirata J., Narisawa N., Ogiwara H., Yamasaki M. Inactivation of food poisoning bacteria and *Geobacillus stearothermophilus* spores by high pressure carbon dioxide treatment // *Food Control*. 2009. V. 20. № 1. P. 53-58.
32. Garcia-Gonzalez L., Geeraerd A.H., Spilimbergo S., Elst K., Van Ginneken L., Debevere J., Van Impe J.F., Devlieghere F. High pressure carbon dioxide inactivation of microorganisms in foods: The past, the present and the future // *International Journal of Food Microbiology*. 2007. V. 117. № 1. P. 1-28.
33. Tomasko D.L., Li H., Liu D., Han X., Wingert M.J., Lee L.J., Koelling K.W. A Review of CO₂ Applications in the Processing of Polymers // *Industrial & Engineering Chemistry Research*. 2003. V. 42. № 25. P. 6431-6456.
34. Menshutina, N.; Abramov, A.; Tsygankov, P.; Lovskaya, D. Extrusion-based 3D printing for highly porous alginate materials production. *Gels* 2021, 7, 92.
35. Menshutina, N.; Abramov, A.; Okisheva, M.; Tsygankov, P. Investigation of the 3D Printing Process Utilizing a Heterophase System. *Gels* 2023, 9, 566. <https://doi.org/10.3390/gels9070566>

Disclaimer/Publisher's Note: The statements, opinions and data contained in all publications are solely those of the individual author(s) and contributor(s) and not of MDPI and/or the editor(s). MDPI and/or the editor(s) disclaim responsibility for any injury to people or property resulting from any ideas, methods, instructions or products referred to in the content.